Plant Physiol. (1992) 100, 1698–1705
0032-0889/92/100/1698/08/$01.00/0

Received for publication April 29, 1992
Accepted September 9, 1992

Kinetics of the Vacuolar H^+-Pyrophosphatase[1]

The Roles of Magnesium, Pyrophosphate, and their Complexes as Substrates, Activators, and Inhibitors

Roger A. Leigh*, Andrew J. Pope[2], Ian R. Jennings, and Dale Sanders

Biochemistry and Physiology Department, Agricultural and Food Research Council Institute of Arable Crops Research, Rothamsted Experimental Station, Harpenden, Hertfordshire AL5 2JQ, United Kingdom (R.A.L., A.J.P.); and Biology Department, University of York, Heslington, York Y01 5DD, United Kingdom (I.R.J., D.S.)

ABSTRACT

The responses of the vacuolar membrane (tonoplast) proton-pumping inorganic pyrophosphatase (H^+-PPase) from oat (*Avena sativa* L.) roots to changes in Mg^{2+} and pyrophosphate (PPi) concentrations have been characterized. The kinetics were complex, and reaction kinetic models were used to determine which of the various PPi complexes were responsible for the observed responses. The results indicate that the substrate for the oat root vacuolar H^+-PPase is Mg_2PPi and that this complex is also a noncompetitive inhibitor. In addition, the enzyme is activated by free Mg^{2+} and competitively inhibited by free PPi. This conclusion differs from that reached in previous studies, in which it was proposed that MgPPi is the substrate for plant vacuolar H^+-PPases. However, models incorporating MgPPi as a substrate were unable to describe the kinetics of the oat H^+-PPase. It is demonstrated that models incorporating Mg_2PPi as the substrate can describe some of the published kinetics of the *Kalanchoë daigremontiana* vacuolar H^+-PPase. Calculations of the likely concentrations of Mg_2PPi in plant cytoplasm suggest that the substrate binding site of the oat vacuolar H^+-PPase would be about 70% saturated in vivo.

It is now well established that the vacuolar membrane (tonoplast) of plant cells possesses two H^+-pumps, one a H^+-ATPase[3], the other a H^+-PPase (10, 14, 21, 22). The reasons for the presence of two H^+ pumps in this membrane remain obscure (14, 22), and, in particular, the role of the H^+-PPase needs to be elucidated. Suggestions thus far include the possibilities (a) that the H^+-PPase acts as a back-up for the H^+-ATPase under conditions in which ATP availability is limiting; (b) that the H^+-PPase is reversible and can use the trans-tonoplast H^+ gradient to synthesize PPi; or (c) that free energy, otherwise dissipated as heat by a soluble PPase, can be conserved as a proton gradient if the H^+-PPase functions in vivo as a pump (14, 22, 29). Insight into the conditions under which the H^+-PPase operates in vivo, and therefore into its function, would be gained if the substrate and other modulators of its activity were known.

In vitro, vacuolar H^+-PPases require both Mg^{2+} and K^+, in addition to PPi, for complete activity (7, 20, 26, 27, 29). However, the response of the enzyme to changes in both $[PPi]_{tot}$ and $[Mg]_{tot}$ can be complex (11, 14, 27, 29). In a reaction medium containing PPi, Mg^{2+}, and K^+, the complexes and ions present include free Mg, free PPi, MgPPi, Mg_2PPi, K^+, and KPPi as well as various protonated forms of the complexes (e.g. 11, 29). This makes it very difficult to test the effect of individual complexes on the activity of the H^+-PPase because the concentration of any single complex cannot easily be changed without altering the concentration of some others. Nonetheless, previous kinetic studies have suggested that the enzyme is activated by both Mg^{2+} and K^+ ions and that the substrate is MgPPi (11, 26, 29). In addition, both free PPi and Mg_2PPi might inhibit the enzyme, although this appears to depend on the tissue from which the tonoplast membranes are prepared (11, 27, 29).

One limitation of the work reported thus far is that the validity of the conclusions drawn from kinetic experiments in vitro has not been tested by quantitative models of the observed data. This paper reports detailed descriptions of the response of the oat (*Avena sativa* L.) root vacuolar H^+-PPase to changes in $[Mg]_{tot}$ and $[PPi]_{tot}$. The data are fitted to reaction kinetic models to elucidate the roles of various PPi complexes. The results suggest that the substrate for the enzyme is Mg_2PPi and that this complex is also a noncompetitive inhibitor. In addition, the enzyme is activated by free Mg and is competitively inhibited by free PPi. We also show that a variant of this model can describe some of the published kinetics of the *Kalanchoë daigremontiana* vacuolar H^+-PPase (29).

MATERIALS AND METHODS

Growth of Plants and Preparation of Tonoplast Vesicles

Seeds of oat (*Avena sativa* L.) cv Trafalgar were germinated and grown in the dark over aerated 0.5 mM $CaSO_4$, and roots were harvested after 5 d. Tonoplast vesicles were prepared

[1] The work of D.S. and I.R.J. was supported by a grant (PG87/501) from the Agricultural and Food Research Council.

[2] Present address: SmithKline Beecham Pharmaceuticals, The Frythe, Welwyn, Hertfordshire, AL6 9AR, United Kingdom.

[3] Abbreviations: H^+-ATPase, vacuolar H^+-translocating ATPase; H^+-PPase, vacuolar H^+-translocating inorganic pyrophosphatase; $[PPi]_{tot}$, $[PPi]_{free}$, $[Mg]_{tot}$, $[Mg]_{free}$, $[Ca]_{tot}$, $[Ca]_{free}$, total and free concentrations of PPi, Mg^{2+}, and Ca^{2+}, respectively; BTP, 1,3-bis[tris(hydroxymethyl)methylamino]-propane.

by separation of microsomal membranes on a 6% (w/w) Dextran-T70 (Pharmacia) step gradient with 250 mM glycerol as the osmoticum (18, 27).

Measurement of H^+-PPase Activity

Hydrolysis of PPi was determined by measuring the release of Pi at 25°C. The reaction mixture (final volume 0.5 mL) contained 250 mM glycerol, 50 mM KCl, 2.5 μg/mL gramicidin-D, 20 mM Hepes-BTP, pH 8.0, and $MgSO_4$ and PPi-BTP at the concentrations indicated. Media (minus vesicles) were preincubated at 25°C and the reaction was started by addition of 50 μL of vesicle suspension containing 2 to 3 μg of protein. Control treatments contained boiled vesicles. Phosphate release was assayed by a modification (18) of the method of Bencini et al. (1). All activities are reported on the basis of mol PPi hydrolyzed (Pi release divided by 2). Tetrasodium PPi was converted to its BTP salt by cation-exchange chromatography with Dowex-50W-X8 resin (H^+ form) and titration with BTP. Calcium concentrations in the solutions were not routinely controlled (cf. ref. 19), but experiments not described here showed that the shape of the response curves to $[Mg]_{tot}$ were not affected when EGTA was included in the assay media.

Measurement of H^+ Transport

Development of an acidic pH within the vesicles was measured fluorometrically with quinacrine as the pH probe using an Aminco-Bowman spectrofluorimeter. The excitation and emission wavelengths were 420 and 495 nm, respectively. The assay medium (final volume 2 mL) contained 250 mM glycerol, 50 mM KCl, 0.35 mM EGTA-BTP, 2 μM quinacrine, 25 mM Hepes-BTP, pH 7.4, and $MgSO_4$ and PPi-BTP at the concentrations indicated. Vesicles (20–50 μg of protein) were preincubated at 25°C in this medium and the reaction was started by the addition of the $MgSO_4$. Initial rates of fluorescence change were calculated from the resultant quench curves.

Protein Determination

Protein was measured by the method of Bradford (3) using BSA as a standard.

Replication

All experiments were performed at least three times, but results are presented from single representative experiments.

Computations

Concentrations of free ions and PPi-metal complexes were calculated using the computer program SOLCON, written by D.C.S. White (University of York) and Y.E. Goldman (University of Pennsylvania). The following dissociation constants were used (17): $[Mg^{2+}][PPi]/[MgPPi]$, $3.63 \cdot 10^{-6}$ M; $[Mg^{2+}]^2[PPi]/[Mg_2PPi]$, $1.66 \cdot 10^{-8}$ M^2; $[Mg^{2+}][H^+][PPi]/[MgHPPi]$, $8.91 \cdot 10^{-13}$ M^2; $[H^+][PPi]/[HPPi]$, $1.12 \cdot 10^{-9}$ M; $[H^+]^2[PPi]/[H_2PPi]$, $8.51 \cdot 10^{-16}$ M^2; $[H^+]^3[PPi]/[H_3PPi]$, $1.35 \cdot 10^{-17}$ M^3; $[H^+]^4$ $[PPi]/[H_4PPi]$, $2.14 \cdot 10^{-18}$ M^4; $[K^+][PPi]/[KPPi]$, $3.98 \cdot 10^{-2}$ M $[K^+][H^+][PPi]/[KHPPi]$, $1.78 \cdot 10^{-10}$ M^2; $[Ca^{2+}][PPi]/[CaPPi]$, $3.98 \cdot 10^{-6}$ M; $[Ca^{2+}][H^+][PPi]/[CaHPPi]$, $5.62 \cdot 10^{-13}$ M^2; $[H^+][EDTA]/[HEDTA]$, $5.50 \cdot 10^{-11}$ M; $[H^+]^2[EDTA]/[H_2EDTA]$, $3.80 \cdot 10^{-17}$ M^2; $[H^{+3}][EDTA]/[H_3EDTA]$, $8.13 \cdot 10^{-20}$ M^3; $[H^+]^4[EDTA]/[H_4EDTA]$, $8.32 \cdot 10^{-22}$ M^4; $[Mg^{2+}][EDTA]/[MgEDTA]$, $2.04 \cdot 10^{-9}$ M; $[Mg^{2+}][H^+][EDTA]/[MgHEDTA]$, $2.88 \cdot 10^{-13}$ M^2; $[Ca^{2+}][EDTA]/[CaEDTA]$, $2.04 \cdot 10^{-11}$ M; $[Ca^{2+}][H^+][EDTA]/[CaHEDTA]$, $1.35 \cdot 10^{-14}$ M^2; $[K^+][EDTA]/[KEDTA]$, $1.58 \cdot 10^{-1}$ M; $[Mg^{2+}][SO_4]/[MgSO_4]$, $5.62 \cdot 10^{-3}$ M; $[K^+][SO_4]/[KSO_4]$, $1.26 \cdot 10^{-1}$ M.

Equations for equilibrium binding models of enzyme activity were derived by standard methods (24) and fitting to experimental data was judged by eye. The fitting strategy for data from any single experiment involved optimizing parameters for a single curve from that experiment and then assessing the fit of the model to other curves from the same experiment. Successful models were those that were judged to give a good description of all curves from an experiment using a single set of enzyme-ligand dissociation constants.

RESULTS

The oat root vacuolar H^+-PPase, whether assayed as PPi hydrolysis or PPi-dependent H^+ transport, showed relatively complex responses to changes in either $[Mg]_{tot}$ or $[PPi]_{tot}$ (Figs. 1 and 2). When $[PPi]_{tot}$ was varied at a fixed $[Mg]_{tot}$ of 5 mM, H^+-PPase activity increased to a maximum at 0.05 to 0.1 mM $[PPi]_{tot}$ and then decreased as $[PPi]_{tot}$ was increased further (Fig. 1). The response to variation in $[Mg]_{tot}$ was almost Michaelian at low fixed $[PPi]_{tot}$, but at higher $[PPi]_{tot}$ activity was low at low $[Mg]_{tot}$ then rose and subsequently fell as $[Mg]_{tot}$ was increased further (Fig. 2). The responses to both

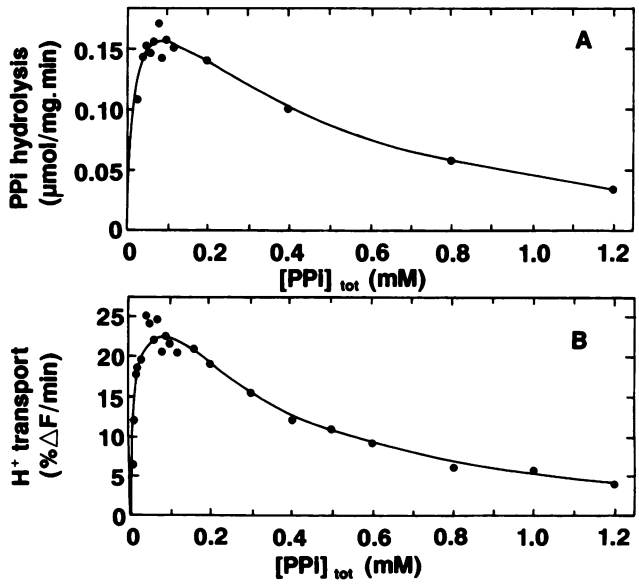

Figure 1. The response of the oat root vacuolar H^+-PPase to changes in $[PPi]_{tot}$ at $[Mg]_{tot}$ = 5 mM. Activity of the H^+-PPase was measured as either PPi hydrolysis (A) or the initial rate of PPi-dependent H^+-transport (B).

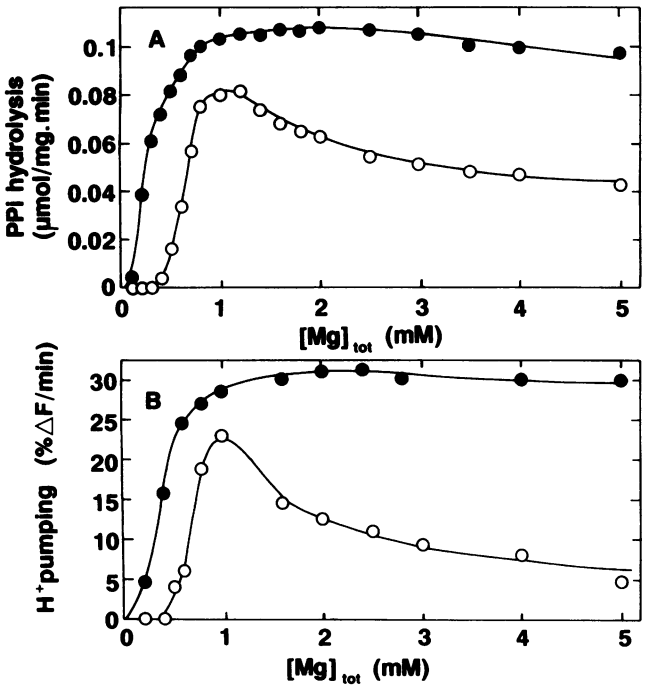

Figure 2. The response of the oat root vacuolar H^+-PPase to changes in $[Mg]_{tot}$ at fixed $[PPi]_{tot}$ of 0.1 (●) or 0.9 (○) mM. Activity of the H^+-PPase was measured as either PPi hydrolysis (A) or the initial rate of PPi-dependent H^+-transport (B).

$[PPi]_{tot}$ and $[Mg]_{tot}$ obviously could not be explained by simple Michaelis-Menten kinetics. However, the number of complexes present in the assay media (see introduction) makes it difficult to analyze the kinetics by controlled changes in the concentration of individual complexes because alterations in the concentration of one complex inevitably affect the concentration of several others. Therefore, we modeled the kinetics numerically.

Initially the modeling concentrated on using MgPPi as the substrate, based on conclusions from earlier studies (11, 26, 29). We also incorporated activation by free Mg for the same reason. However, we were unable successfully to describe the data using such a simple model (not shown). We further modified the model by incorporating competitive inhibition by free PPi or noncompetitive inhibition by Mg_2PPi, but although these give some improvement, the fits are still inadequate (e.g. Fig. 3). In particular, the models fail to describe the changes in activity at low $[Mg]_{tot}$ with various fixed $[PPi]_{tot}$. A more detailed analysis of the changes in the concentration of MgPPi and in $[Mg]_{tot}$ revealed that this is because the increases in concentrations of these ligands are too small to account for the changes in activity. For instance, with a fixed $[PPi]_{tot}$ of 1.5 mM, H^+-PPase activity increased 50-fold when $[Mg]_{tot}$ increased from 0.4 to 1.4 mM, but MgPPi increased only 3-fold and free Mg, 9-fold. Thus, if the reaction is first order with respect to each ligand, the combined changes in concentration could account for only a 27-fold increase in H^+-PPase activity. However, a similar analysis for Mg_2PPi and free Mg indicated that the combined increase in concentrations was 240-fold, more than adequate to account for the observed change in activity if Mg_2PPi is the substrate. Therefore, we next examined whether models incorporating Mg_2PPi as the substrate would provide a better description of the data.

Again, initial attempts to model the data with a two-site model with Mg_2PPi as the substrate and free Mg as an activator were unsuccessful (not shown). We increased the complexity and found one model that was able to fit the data adequately. A schematic representation of the model is shown in Figure 4. The left-hand cube of the model represents random equilibrium binding of substrate (S = Mg_2PPi), or noncompetitive inhibitor (I = Mg_2PPi) to the enzyme, and the right-hand cube represents random binding of the competitive inhibitor, free PPi. The move from the lower to the upper plane represents random equilibrium binding of free Mg. The relevant equilibrium constants are modified (indicated by the Greek letters) to ensure microscopic reversibility, a thermodynamic requirement. Hydrolysis of substrate can only occur when free Mg is bound (upper plane of model). To obtain good fits it was necessary to make the EISMg complex catalytically competent, and the proportion of hydrolysis of substrate via this complex is varied by changing the value of the parameter a.

The result of fitting the model to data from an experiment in which response of the H^+-PPase to $[Mg]_{tot}$ was measured at four different fixed $[PPi]_{tot}$ is shown in Figure 5. The model provides a good description of the data. The results indicate that the low activity measured with low $[Mg]_{tot}$ (<0.5 mM) at relatively high fixed $[PPi]_{tot}$ (1.5 mM) is due to the combined effects of low substrate concentration, competitive inhibition

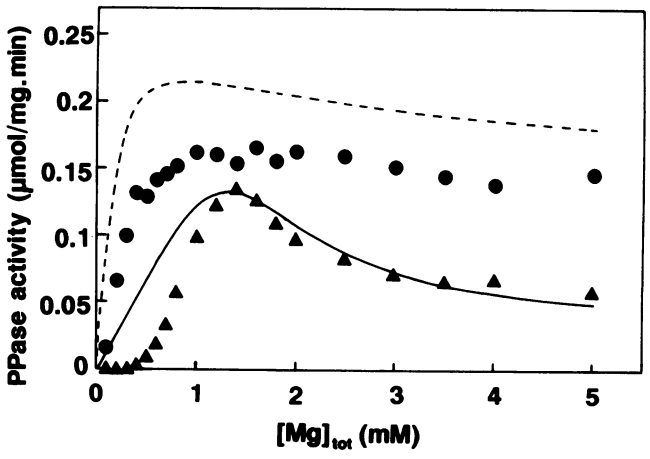

Figure 3. Fit of a model incorporating MgPPi as the substrate, activation by free Mg, and noncompetitive inhibition by Mg_2PPi to data from an experiment measuring the response of the oat root vacuolar H^+-PPase to variations in $[Mg]_{tot}$ at fixed $[PPi]_{tot}$ of 0.1 (●) or 1.5 mM (▲). Activity of the H^+-PPase was measured as PPi hydrolysis. The model was similar to that in Figure 4 except that competitive inhibition by free PPi was not assumed. Symbols indicate experimental data, lines the fitted model. Parameters used in the model are defined in Figure 4 and for this fitting exercise had the values V_{max} = 0.29 µmol mg^{-1} of protein min^{-1}; K_S = 5 µM; K_{Mg} = 90 µM; K_I = 90 µM; a = 0; $\alpha = \beta = \gamma = \delta = \epsilon = 1$. S, MgPPi; I, Mg_2PPi.

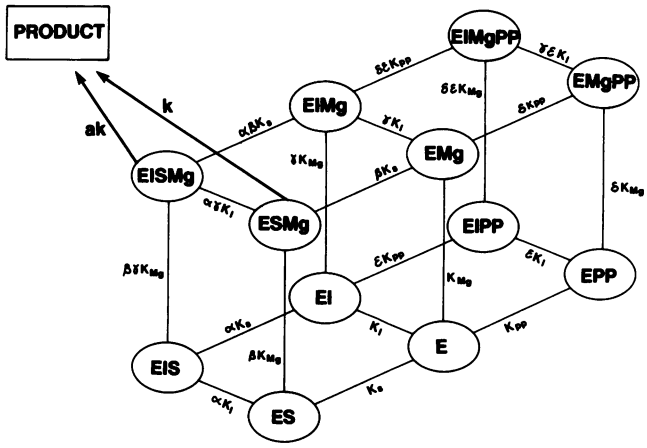

Figure 4. Schematic representation of the model used successfully to describe the kinetics of the oat root vacuolar H+-PPase. For the relationships shown in Figures 5 through 7, the identifiers are S, Mg_2PPi; Mg, free Mg; I, Mg_2PPi; and PP, free PPi. In the poorer fits of Figure 3, MgPPi replaces Mg_2PPi as S. Details of the equations that describe this model mathematically are given in the Appendix.

by free PPi, and insufficient free Mg to activate the enzyme. The fall in activity at high $[Mg]_{tot}$ is due to noncompetitive inhibition by Mg_2PPi. This decrease in activity is relatively small in the presence of 0.1 mM $[PPi]_{tot}$ because the concentration of Mg_2PPi in these conditions does not rise above 41 μM.

To test the model further we examined its ability to describe data derived from a second, independent experiment in which the response of the H+-PPase to $[PPi]_{tot}$ was determined at different fixed $[Mg]_{tot}$. Again the model provides a good description of the data (Fig. 6). A particularly rigorous test of the model is its ability to describe the rise and fall in activity as $[PPi]_{tot}$ increases in the presence of 1.5 mM $[Mg]_{tot}$. The modeling indicates that with this $[Mg]_{tot}$, the changes in activity between 0.1 and 2.0 mM $[PPi]_{tot}$ are inversely related to the changes in Mg_2PPi concentration, whereas the subsequent decline up to 3 mM $[PPi]_{tot}$ is due to decreases in free Mg as it all becomes complexed with PPi. The model also adequately predicts the observation that activity measured in the presence of 5 mM $[Mg]_{tot}$ is lower than that measured with 1.5 mM $[Mg]_{tot}$. This is because inhibition by Mg_2PPi is greater at the higher $[Mg]_{tot}$. Comparison of the model parameter values for the independent experiments in Figures 5 and 6 shows that the fits to the two sets of data require changes no greater than 2-fold in the dissociation constants for S, I, free Mg, and free PPi.

As a further test of the model, we examined whether it could describe the data of White et al. (29) for the response of the vacuolar H+-PPase from *K. daigremontiana* to variations in $[Mg]_{tot}$. As indicated in the introduction, these authors concluded that this H+-PPase uses MgPPi as its substrate. Nonetheless, a model based on that in Figure 4 and using Mg_2PPi as the substrate was able to describe adequately the response of the *Kalanchoë* H+-PPase to variations in $[Mg]_{tot}$ between 0 and 10 mM (Fig. 7). As well as using Mg_2PPi as the substrate, the model also includes activation by free Mg and competitive inhibition by free PPi but not inhibition by Mg_2PPi. Fits to the data at the larger values of $[Mg]_{tot}$ (>3 mM) were less good but measured activities in this region were quite variable (e.g. data for 0.5 mM $[PPi]_{tot}$). Attempts were also made to model data from another experiment

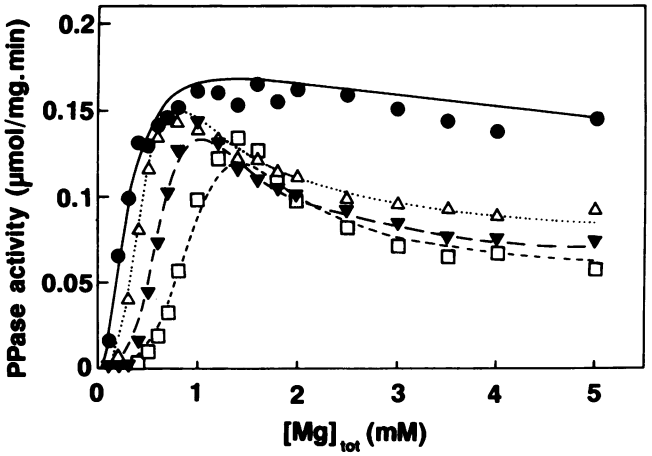

Figure 5. Description of the response of the oat root vacuolar H+-PPase to variation in $[Mg]_{tot}$ by a model incorporating Mg_2PPi as the substrate, activation by free Mg, noncompetitive inhibition by Mg_2PPi, and competitive inhibition by free PPi. The experiment is the same as in Figure 3 but shows the complete data set for the effects of variation in $[Mg]_{tot}$ at fixed $[PPi]_{tot}$ of 0.1 (●), 0.5 (△), 0.9 (▼), and 1.5 (□) mM. Symbols indicate experimental data, whereas lines are the fitted model. Parameter values were V_{max} = 0.29 μmol mg^{-1} of protein min^{-1}; K_S = 5 μM; K_{Mg} = 25 μM; K_I = 700 μM; K_{PP} = 150 μM; a = 0.15; α = 0.55; γ = 0.1; $\beta = \delta = \epsilon = 1$.

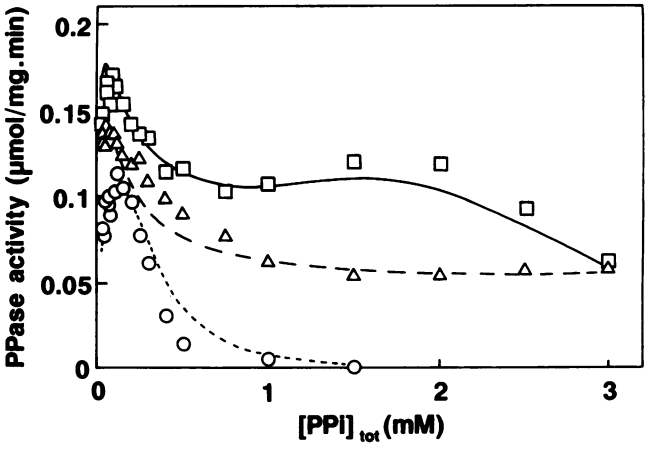

Figure 6. Description of the response of the oat root vacuolar H+-PPase to variation in $[PPi]_{tot}$ by a model incorporating Mg_2PPi as the substrate, activation by free Mg, noncompetitive inhibition by Mg_2PPi, and competitive inhibition by free PPi. Activity of the H+-PPase was measured as PPi hydrolysis in the presence of various $[PPi]_{tot}$ at fixed $[Mg]_{tot}$ of 0.25 (○), 1.5 (□), and 5.0 (△) mM. Symbols indicate experimental data, lines the fitted model. Parameter values were V_{max} = 0.28 μmol mg^{-1} of protein min^{-1}; K_S = 2.5 μM; K_{Mg} = 25 μM; K = 600 μM; K_{PP} = 100 μM; a = 0.15; α = 0.55; γ = 0.1; $\beta = \delta = \epsilon = 1$.

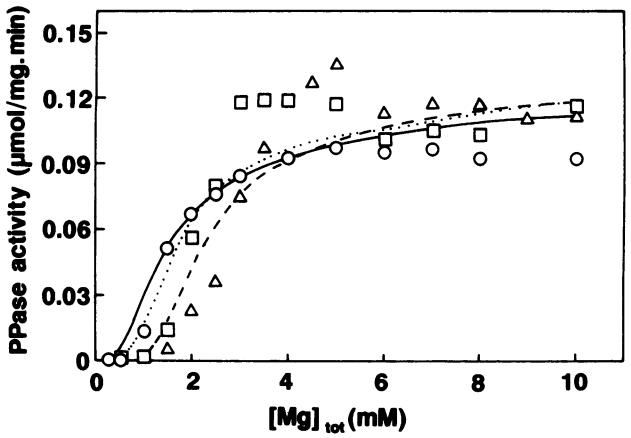

Figure 7. Description of the response of the *Kalanchoë* vacuolar H^+-PPase to variation in $[Mg]_{tot}$ by a model incorporating Mg_2PPi as the substrate, activation by free Mg, and competitive inhibition by free PPi. The data (from figure 2A of ref. 29) are indicated by the symbols and the fitted kinetics by the lines. The $[PPi]_{tot}$ used were 0.1 (O, solid line), 0.5 (□, dashed line), and 1.0 mM (▲, dotted line). Parameter values were V_{max} = 0.14 µmol mg^{-1} of protein min^{-1}; K_S = 5 µM; K_{Mg} = 800 µM; K_{PP} = 10 µM; $a = 0$; $\alpha = \beta = \gamma = \delta = \epsilon = 1$.

(figure 6 in ref. 29), which showed that the activity of the *Kalanchoë* H^+-PPase declined as $[Mg]_{tot}$ increased from 10 to 100 mM. However, we were unable to obtain good fits to these data. A possible explanation for this is given below.

DISCUSSION

As found previously (14, 18, 27), the oat root vacuolar H^+-PPase displays complicated kinetics in response to changes in $[Mg]_{tot}$ or $[PPi]_{tot}$. The large number of PPi complexes that can potentially interact with the enzyme to produce these responses precludes an analysis of the kinetics by the usual approach of varying the concentration of a single complex while maintaining all others constant. Therefore, the results were analyzed using reaction kinetic models. The outcome indicates that the substrate for the oat root vacuolar H^+-PPase is Mg_2PPi. This complex is also a noncompetitive inhibitor of the enzyme, whereas free Mg activates and free PPi competitively inhibits. Models that incorporate MgPPi as the substrate cannot describe the data, in contrast with previous suggestions that this is the substrate of the vacuolar H^+-PPase in plants (11, 26, 29). However, the previous studies did not undertake quantitative modeling of H^+-PPase kinetics.

A model incorporating Mg_2PPi as the substrate is able to describe some, but not all, of the kinetics of the *Kalanchoë* H^+-PPase (Fig. 7). In particular, we could not use the model to explain the decrease in the activity of the *Kalanchoë* H^+-PPase as $[Mg]_{tot}$ was increased from 10 to 100 mM in the presence of 0.1 mM $[PPi]_{tot}$ (see figure 6 in ref. 29). This decline in activity was accompanied by an increase in Mg_2PPi and a decrease in MgPPi, and White et al. (29) concluded that this strongly supported the notion that MgPPi is the substrate. However, an alternative explanation is that the kinetics are a response to changes in contaminating $[Ca]_{free}$. Low concentrations of this ion cause substantial inhibition of the vacuolar H^+-PPase from *Vigna* and *Beta* (16, 19). White et al. (29) measured their activities in the presence of 0.3 mM EDTA because this stimulated activity and they explained this stimulation on the basis of chelation of Ca^{2+} contaminating the assay media, although no measurements of $[Ca]_{free}$ were made. If Ca^{2+} was present, then the extent of its chelation by EDTA would depend on the Mg^{2+} concentration. Therefore, we used the SOLCON program to calculate whether it was possible that changes in $[Ca]_{free}$ could explain the decrease in H^+-PPase activity as $[Mg]_{tot}$ was increased from 10 to 100 mM. The calculations show that if the solutions used by White et al. (29) contained 5 µM $[Ca]_{tot}$, the $[Ca]_{free}$ would have changed from 0.8 to 2.2 µM as $[Mg]_{tot}$ increased from 10 to 100 mM. A plot of the H^+-PPase activity measured by White et al. (29) against this change in $[Ca]_{free}$ shows that the two are inversely related (Fig. 8), suggesting that free Ca could have inhibited the enzyme. Because no measurements of $[Ca]_{free}$ were made on the solutions used by White et al. (29), this explanation is obviously speculative. Nonetheless, the relationship in Figure 8 and the ability of a model with Mg_2PPi as the substrate (Fig. 7) to describe some of the data of White et al. (29) suggest that some doubt must remain about the conclusion that MgPPi is the substrate for the *Kalanchoë* vacuolar H^+-PPase. It is interesting that the model fitted the *Kalanchoë* data without the need to invoke inhibition by Mg_2PPi, which may indicate substantial interspecific variation in this property. The reason for such differences, if they are confirmed, remains unclear.

The finding that Mg_2PPi is the substrate of the oat root vacuolar H^+-PPase suggests that this PPase is distinct from other well-characterized PPases, for which there is good kinetic evidence in favor of MgPPi as the substrate (e.g. 6, 25). However, Mg_2PPi has been shown to be a substrate for the low-activity, T-form of the *Streptococcus faecalis* PPase (13). In addition, a number of soluble PPases that use MgPPi

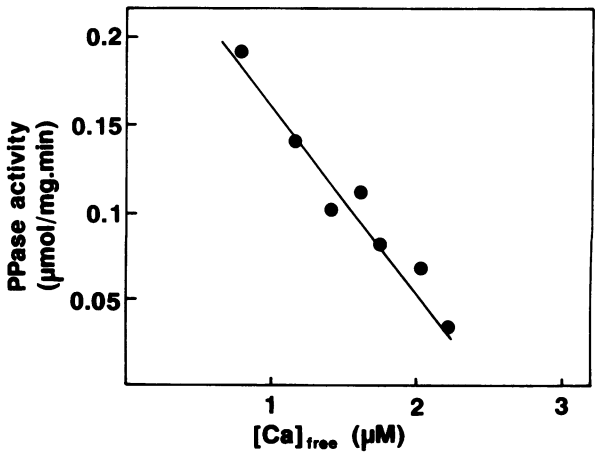

Figure 8. The derived relationship between the activity of the *Kalanchoë* vacuolar H^+-PPase activity and free Ca. The H^+-PPase activities are from the experiment described in figure 6 of ref. 29. The program SOLCON was used to calculate the $[Ca]_{free}$ in solutions used in the experiment, assuming that they contained a $[Ca]_{tot}$ of 5 µM.

as their substrate require a further two Mg^{2+} ions to be bound for maximal activity (6, 25). The binding of a single Mg^{2+} ion and a further two complexed to Mg_2PPi to the oat vacuolar H^+-PPase indicates that this enzyme has the same operational requirement as other PPases for three Mg^{2+} ions to be bound per active site.

The question arises as to whether the concentration of Mg_2PPi in plant cells is sufficiently large to allow the vacuolar H^+-PPase to be active in vivo. The concentration of $[PPi]_{tot}$ in the cytoplasm is thought to be relatively constant at 0.2 to 0.3 mM (28), but $[Mg]_{free}$ is not known with accuracy; the only measurement in plants suggests a value of 0.4 mM (30). In animal cells, $[Mg]_{free}$ ranges from 0.4 to 3.5 mM (2, 9). We have calculated the concentrations of MgPPi, Mg_2PPi, and free PPi that would be present in plant cell cytoplasm containing 0.25 mM $[PPi]_{tot}$, 0.4 or 3.5 mM $[Mg]_{free}$, and 100 mM K^+ (15) with a pH of 7.2 (8). With 0.4 mM $[Mg]_{free}$, the concentration of MgPPi is 94 μM, nearly 12-fold higher than that of Mg_2PPi, which is only 8 μM, whereas $[PPi]_{free}$ is 72 μM (Table I). With 3.5 mM $[Mg]_{free}$, MgPPi increases by only 18%, whereas Mg_2PPi concentration increases 10.6-fold to 85 μM and $[PPi]_{free}$ decreases to 10 μM. Substituting these values into the model indicates that under both sets of conditions the H^+-PPase would operate at about 70% of the maximum activity measured in vitro. Highest activities (94% of maximum measured in vitro) would be achieved if the cytoplasm contains about 0.8 mM $[Mg]_{free}$ (Table I). These data indicate that high rates of activity are possible under physiological conditions with Mg_2PPi as the substrate.

It is thought that the vacuolar H^+-PPase may be a multisubunit enzyme (5, 23). This raises the possibility that the enzyme shows cooperative kinetics with respect to certain complexes, and it has been proposed that binding of free Mg to the *Kalanchoë* H^+-PPase is cooperative (29). We have not explicitly considered such models, but we have found that a noncooperative model could explain some of the kinetics of the *Kalanchoë* H^+-PPase (Fig. 7), thus demonstrating that cooperativity is not the only explanation for the observed kinetics. It is quite possible that cooperative models could be found that could fit the data for the oat root tonoplast H^+-PPase. However, it is unlikely that the fits would be better than those obtained with the multiple binding site model in Figure 4, and the modeling would be unable to distinguish which of several possibilities is the real description of the kinetics. Therefore, the best approach now would seem to be further biochemical investigations to determine whether evidence for or against the proposed model can be found.

The model we tested assumes that each of the complexes interacting with the H^+-PPase requires a different binding site (Fig. 4), thereby indicating a minimum of three different binding sites: the active site binding Mg_2PPi competitively with free PPi, an inhibitory site binding Mg_2PPi, and a free Mg binding site. In addition, it is known that the enzyme requires K^+ for complete activity (7, 26, 27, 29), which indicates a fourth binding site, and Ca^{2+} inhibition can only be explained if there is a separate binding site for this ion (19). Therefore, there must be at least five separate binding sites on the enzyme. However, structural evidence for the existence of these sites is lacking. Mixtures of Mg^{2+} and PPi will protect the vacuolar H^+-PPase from inhibition by residue-specific inhibitors such as *N*-ethylmaleimide, phenylglyoxal, and 2,3-butanedione (4, 12). This suggests that MgPPi or Mg_2PPi is protecting the enzyme by binding at a specific site, presumably the active site. However, the complex providing protection has not been positively identified. The investigation of such protective effects of various PPi complexes might provide direct evidence for one or more of the proposed binding sites required by the model proposed in this paper.

APPENDIX

The rate equation for the model in Figure 4 can be derived by assuming equilibrium binding of ligands with the enzyme (E), in conjunction with catalytic competence of selected ligand-bound forms of the enzyme. For the model in Figure 4, we can write:

$$\frac{v}{E_t} = \frac{[ESMg]k + [EISMg]ak}{[E] + [ES] + [EI] + [EMg] + [EIS] + [ESMg] + [EIMg] + \ldots}, \quad (1)$$

where v is the velocity (enzyme activity), E_t is the total concentration of enzyme, a represents the relative rate of hydrolysis of the [EISMg] complex, and the denominator of

Table I. *Concentrations of PPi Complexes and Calculated Activity of the Vacuolar H^+-PPase in Cytoplasmic Conditions*

The program SOLCON was used to calculate the concentrations of PPi complexes in a cytoplasm containing 0.25 mM $[PPi]_{tot}$, 100 mM $[K^+]$, 0.4, 0.82, or 3.5 mM $[Mg]_{free}$, with a pH of 7.2. Concentrations of $[Mg]_{tot}$ were adjusted until the required $[Mg]_{free}$ were achieved. Activities of H^+-PPase were calculated using the parameters in Figure 5 and expressed relative to the maximum activity measured in the experiment in Figure 5.

Concentration of Complex				H^+-PPase Activity
$[Mg]_{free}$	[MgPPi]	$[Mg_2PPi]$	$[PPi]_{free}$	
mM	μM	μM	μM	% maximum
0.40	94	8	72	76
0.82	118	21	44	94
3.50	111	85	10	69

the right-hand side comprises the concentrations of all forms of the enzyme.

Dissociation constants are defined as

$$K_s = [E][S]/[ES];\ K_I = [E][I]/[EI];\ \text{etc.}$$

The Greek letters α through ϵ (see Fig. 4) are introduced to ensure microscopic reversibility, which is a thermodynamic prerequisite. This results in dissociation constants for the ternary forms of the enzyme as

$$\alpha K_s = [E][I][S]/[EIS]K_I;\ \beta K_{Mg} = [E][S][Mg/[ESMg]K_s;\ \text{etc.}$$

and for the quaternary forms as

$$\alpha\beta K_s = [E][I][S][Mg]/[EISMg]\gamma K_{Mg}K_I,\ \text{etc.}$$

Substituting into Equation 1, defining $V_{max} = E_t k$, and rearranging yields

$$v = \text{NUM/DEN} \qquad (2)$$

where the numerator is defined as

$$NUM = \frac{V_{max}[S][Mg]}{\beta K_s K_{Mg}}\left[1 + \frac{[I]a}{\alpha\delta K_I}\right]$$

and the denominator as

$$DEN = 1 + \frac{[Mg]}{K_{Mg}}\cdot Q + \frac{[S]}{K_s}\left[1 + \frac{[I]}{\alpha K_I}\right] + \frac{[PP]}{K_{PP}}\left[1 + \frac{[Mg]}{\delta K_{Mg}}\right] + \frac{[I]}{K_I}\left[1 + \frac{[PP]}{\epsilon K_{PP}}\right]$$

with

$$Q = 1 + \frac{[S]}{\beta K_s}\left[1 + \frac{[I]}{\alpha\gamma K_I}\right] + \frac{[I]}{\gamma K_I}\left[1 + \frac{[PP]}{\delta\epsilon K_{PP}}\right]$$

Equation 2 therefore defines the response of the model in Figure 4 to variation in ligand concentration, providing that the dissociation constants, the relative rates of hydrolysis of the catalytically active forms, the constants defining microscopic reversibility, and the V_{max} (which acts simply as a scaling factor) are specified.

ACKNOWLEDGMENTS

We thank Drs. P.J. White (Horticulture Research Internations, East Malling, UK) and J.A.C. Smith (University of Oxford) for providing us with the original data for their studies of the vacuolar H^+-PPase from *Kalanchoë* and for helpful discussions throughout the course of this work.

LITERATURE CITED

1. **Bencini DA, Wild JR, O'Donovan GA** (1983) Linear one-step assay for the determination of orthophosphate. Anal Biochem **132:** 254–258
2. **Blatter LA, McCuigan JAS** (1988) Estimation of the upper limit of the free magnesium concentration measured with Mg-sensitive microelectrodes in ferret ventricular muscle: (1) use of the Nicolsky-Eisenman equation and (2) in calibrating solutions of the appropriate concentration. Magnesium **7:** 154–165
3. **Bradford MM** (1976) A rapid and sensitive method for the quantitation of microgram quantities of protein utilizing the principle of protein dye-binding. Anal Biochem **72:** 248–256
4. **Britten CJ, Turner JC, Rea PA** (1989) Identification and purification of substrate binding subunit of higher plant H^+ translocating inorganic pyrophosphatase. FEBS Lett **256:** 200–206
5. **Chanson A, Pilet P-E** (1989) Target molecular size and sodium dodecyl polyacrylamide gel electrophoresis analysis of the ATP- and pyrophosphate-dependent proton pumps from maize root tonoplast. Plant Physiol **90:** 934–938
6. **Cooperman BS** (1982) The mechanism of action of yeast inorganic pyrophosphatase. Methods Enzymol **87:** 526–548
7. **Davies JM, Rea PA, Sanders D** (1991) Vacuolar proton-pumping pyrophosphatase in *Beta vulgaris* shows vectorial activation by potassium. FEBS Lett **278:** 66–68
8. **Felle H, Bertl A** (1986) The fabrication of H^+-selective liquid-membrane micro-electrodes for use in plant cells. J Exp Bot **37:** 1416–1428
9. **Flatman PW** (1991) Mechanisms of magnesium transport. Annu Rev Physiol **53:** 259–271
10. **Hedrich R, Kurkdjian A, Guern J, Flügge UI** (1989) Comparative studies of the electrical properties of the H^+-translocating ATPase and pyrophosphatase of the vacuolar-lysosomal compartment. EMBO J **8:** 2835–2841
11. **Johannes E, Felle HH** (1989) The role of Mg^{2+} in proton transport by the tonoplast pyrophosphatse of *Riccia fluitans* vacuoles. Physiol Plant **77:** 326–331
12. **Kuo SY, Pan RL** (1990) An essential arginyl residue in the tonoplast pyrophosphatase from etiolated mung bean seedlings. Plant Physiol **93:** 1128–1133
13. **Lahti R, Jokinen M** (1985) Kinetic model for the action of the inorganic pyrophosphatase from *Streptococcus faecalis*. Biochemistry **24:** 3526–3530
14. **Leigh RA, Pope AJ** (1987) Understanding tonoplast function: some emerging problems. *In* B Marin, ed, Plant Vacuoles: Their Importance in Solute Compartmentation in Cells and Their Applications in Plant Biotechnology. Plenum Press, New York, pp 101–110
15. **Leigh RA, Wyn Jones RG** (1984) A hypothesis relating critical potassium concentrations for growth to the distribution and functions of this ion in the plant cell. New Phytol **97:** 1–13
16. **Maeshima M** (1991) H^+ translocating inorganic pyrophosphatase of plant vacuoles. Inhibition by Ca^{2+}, stabilization by Mg^{2+} and immunological comparison with other pyrophosphatases. Eur J Biochem **196:** 11–17
17. **Martell AE, Smith R** (1976) Critical Stability Constants, Vol 1. Plenum Press, New York
18. **Pope AJ, Leigh RA** (1987) Some characteristics of anion transport at the tonoplast of oat roots, determined from the effects of anions on pyrophosphate-dependent proton transport. Planta **172:** 91–100
19. **Rea PA, Britten CJ, Jennings IR, Calvert CM, Skiera L, Leigh RA, Sanders D** (1992) Regulation of vacuolar H^+-pyrophosphatase by free calcium. A reaction kinetic analysis. Plant Physiol **100:** 1706–1715
20. **Rea PA, Poole RJ** (1985) Proton-translocating inorganic pyrophosphatase of red beet (*Beta vulgaris* L.) tonoplast vesicles. Plant Physiol **77:** 46–52
21. **Rea PA, Poole RJ** (1986) Chromatographic resolution of H^+-translocating pyrophosphatase from H^+-translocating ATPase of higher plant tonoplast. Plant Physiol **81:** 126–129
22. **Rea PA, Sanders D** (1987) Tonoplast energization: two pumps, one membrane. Physiol Plant **71:** 131–141
23. **Sarafian V, Poole RJ** (1989) Purification of an H^+-translocating inorganic pyrophosphatase from vacuole membranes of red beet. Plant Physiol **91:** 34–38
24. **Segel IH** (1975) Enzyme Kinetics: Behaviour and Analysis of Rapid Equilibrium and Steady State Enzyme Systems. John Wiley & Sons, New York

25. **Unguryte A, Smirnova IN, Baykov AA** (1989) Kinetic models for the action of cytosolic and mitochondrial inorganic pyrophosphatase of rat liver. Arch Biochem Biophys **273:** 292–300
26. **Walker RR, Leigh RA** (1981) Mg^{2+}-dependent, cation-stimulated inorganic pyrophosphatase associated with vacuoles isolated from storage roots of red beet (*Beta vulgaris* L.). Planta **153:** 150–155
27. **Wang Y, Leigh RA, Kaestner KH, Sze H** (1986) Electrogenic H^+-pumping pyrophosphatase in tonoplast vesicles of oat roots. Plant Physiol **81:** 497–502
28. **Weiner H, Stitt M, Heldt HW** (1987) Subcellular compartmentation of pyrophosphate and alkaline pyrophosphatase in leaves. Biochim Biophys Acta **893:** 13–21
29. **White PJ, Marshall J, Smith JAC** (1990) Substrate kinetics of the tonoplast H^+-translocating inorganic pyrophosphatase and its activation by free Mg^{2+}. Plant Physiol **93:** 1063–1070
30. **Yazaki Y, Asukagawa N, Ishikawa Y, Ohta E, Sakata M** (1988) Estimation of cytoplasmic free Mg^{2+} levels and phosphorylation potentials in mung bean root tips by in vivo ^{31}P NMR spectroscopy. Plant Cell Physiol **29:** 919–924